T.3: Development of GaN ultra-violet photodetector for application in a harsh radiation environment

Abhishek Chatterjee
Materials Science Section
Email: cabhishek@rrcat.gov.in

Abstract
Recent advances in nitride semiconductors have led to significant progress in the development of GaN-based optoelectronic devices including light-emitting diodes, lasers, and detectors. In this context, development of high-performance GaN-based ultraviolet (UV) photodetectors (PDs) for potential application in a high-radiation environment have been carried out. Due to the hetero-epitaxial growth of GaN on foreign substrates, considerable lattice mismatch exists between the epilayer and substrate that results in a large density of threading dislocations in GaN. These line defects offer an additional highly conductive path to the carriers for transport across metal/semiconductor Schottky junction-based PDs via dislocation-assisted tunneling. In this article, the role of dislocation on the optoelectronic properties of the GaN epitaxial layer and Schottky junction-based GaN UV detector is presented. Unique methods to control the carrier tunneling and enhance the detector performance have been demonstrated for device-specific applications. Finally, the performance of the fabricated device was tested under ^{60}Co Gamma irradiation where a fast self-recovery of the device response within a day after irradiation signifies its compatibility for operation in high radiation zones.

1. Introduction

Semiconductor optoelectronic devices based on GaN have led to a significant progress recently, which results in the development of GaN based UV PDs for light detection in the spectral range of 280 nm to 360 nm. Such detectors are important for many applications including visible blind UV detection, usage in strategic sectors, UV astronomy, and medical science and also in the industry as flame detectors and solar UV monitors [1]. Due to their visible blind nature, radiation-resistance and thermal stability, these devices offer several advantages over conventional photomultiplier tubes and Si-based UV detectors [2]. Compared to Si-based devices, nitride devices are more radiation tolerant because of a high displacement energy. Also the leakage current of GaN PDs is lower as compared to Si due to wider band gap, which clearly demonstrates a high radiation resistance of GaN. It makes GaN a suitable candidate for potential applications in the harsh environments of nuclear reactors, particle accelerators and spacecraft [3].

Although great achievements have been made in GaN based optoelectronic devices, there are several challenges in growing good quality GaN epilayers. In general, GaN based epitaxial layers are grown by two techniques namely, Hydride Vapour Phase Epitaxy (HVPE) and Metal Organic Vapour Phase Epitaxy (MOVPE) [4,5].

The lack of a suitable substrate for GaN is the first and foremost difficulty in growing high crystalline quality. Among all the foreign substrates like sapphire, SiC and silicon, sapphire is the primary choice for growing GaN due to its availability, low cost, surface morphology and high temperature stability compared to other substrates, irrespective of having a large lattice mismatch of ~14% with GaN [6]. However, such a large lattice mismatch leads to high density of threading dislocations in epilayers usually in the range of ~10^{9}–10^{11} cm^{-2} [7]. A major consequence of this appears in terms of a large n-type conductivity of GaN epilayers due to the unintentional doping by residual impurities such as silicon and oxygen. However, in order to optimize the performance of optoelectronic devices, the dopant density of constituent layers needs to be controlled with good precision. In a highly defective material system like GaN/sapphire, a careful assessment of the electronic transport parameters such as carrier mobility, background carrier density, leakage current is mandatory prior to the development of a working device. Significant efforts have been made by many researchers for reducing the density of threading dislocations by incorporating low temperature grown buffer layers [8], SiNx interlayer [9], substrate patterning, and innovative surface treatments of the substrate. Irrespective of the progress reported via such attempts and the corresponding development of novel nitride devices, GaN epilayers still possess a large density of threading dislocations [10] that substantially contributes to the leakage current in nitride devices [5].

This work deals with the fabrication of high performance GaN based UV PDs for potential application in high radiation environments. A reasonable control of the dislocation formation during epitaxial growth and a knowledge of dislocation behaviour are the two pre-requisite for optimizing the performance of a nitride device. The two issues addressed here are: (1) epitaxial growth of GaN is presented by highlighting the problems related to dislocation density, and (2) the role of dislocations in the performance of GaN-based radiation hard UV PDs. In particular, results from the metal-semiconductor-metal (MSM) and metal-oxide-semiconductor (MOS) configurations of GaN PDs are presented, where a state-of-the-art performance of GaN based MOS devices is demonstrated. Systematic electronic transport measurements have been performed to understand the fundamental mechanisms associated with current conduction in GaN epilayers. A few samples have also been tested under a high dose of ^{60}Co gamma rays, which proves the radiation resistant nature of indigenously developed GaN devices along with a fast self-recovery and thereby signifies their usefulness for possible applications in harsh radiation environment.

2. Experimental details

GaN epitaxial layers are grown on 2 inch sapphire substrate by HVPE and MOVPE techniques. Thickness of GaN epilayers is 5 µm and the layers are n-type doped. The samples are cut into square pieces (5×5 mm^2) from 2 inch epilayer and Ohmic contacts are made with indium metal by rapid thermal annealing at 375 °C for 40 s in nitrogen ambient. Carrier concentration and mobility values for each sample are

measured using Hall technique [11]. The measurement set up is shown in Figure T.3.1(a) and the detailed measurement procedure is discussed elsewhere [12]. Capacitance–voltage (C-V) measurements are performed to extract the carrier concentration as a function of temperature, where Ni (15 nm)/Au (100 nm) Schottky contacts were fabricated on top GaN surface. A Keithley 590 analyzer operated at 1 MHz was used to measure the C–V characteristics. The current-voltage (I–V) characteristics measured in dark and under illumination with a 325 nm UV laser and transient photocurrent measurements are carried out using the Keithley 2450 source meter. The Hall and C-V/V-I measurement are performed in configuration 1 and 2 as shown in Figure T.3.1 (b) Furthermore, the room temperature photo-response measurements are carried out using a 100 W xenon lamp (excitation source), a 320 mm focal length monochromator, and a lock-in amplifier as shown in Figure T.3.1(c). A 325 nm He–Cd laser is also used for the measurement of responsivity and transient response of the PDs.

3. Effect of dislocation in GaN epitaxial layer

In order to realize the impact of dislocation on the electrical transport properties in GaN epitaxial layer, measurements are meticulously carried out on 5 µm thick GaN/Sapphire epilayers grown by HVPE and MOVPE. It is found that though the two samples possess a carrier density of ~2×10^{18} cm^{-3}, their origin is very different. It is observed that the carrier concentration measured by Hall for HVPE grown samples is two orders larger than the value provided by C-V technique as shown in Figure T.3.2(a). Such a large difference in carrier concentration is associated with the formation of a degenerate layer at the layer-substrate interface, which consisted of a large density of threading screw and edge dislocations [10]. A two layer model is used to extract the appropriate values of carrier concentration of HVPE grown samples from Hall data as shown in Figure T.3.2(b). Furthermore, although the corrected carrier concentration and mobility graphs has a regular shape [13], the corrected carrier concentration are still 2 orders larger than the C-V values at room temperature. Gotz et al. [14] have also studied HVPE GaN epitaxial layers by Hall and C-V techniques where they have found one order difference between the carrier concentration values for 13 and 7 µm thick GaN layers. Further, a difference of ~3 orders was observed for 1.2 µm thick GaN layer. In order to understand this point, the carrier concentration values measured by several researchers are plotted along with our values in Figure T.3.2(b). Here, trends are clearly observed, where the difference between carrier concentration values measured by the Hall and C-V techniques reduces at large thickness of GaN epilayer. It is learnt that there exists a critical thickness for HVPE GaN epilayers below which the electronic transport properties of layers grown on top of them are severely limited by the interfacial charged dislocations as shown by the inset of Figure T.3.2(b).

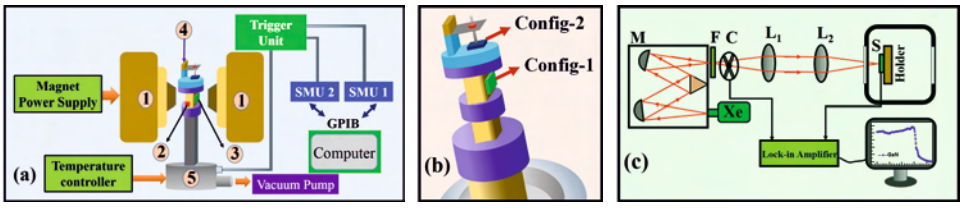

Fig. T.3.1: (a) Schematic of the experimental set up showing- (1) magnet pole pieces, (2) sample heater, (3) sample, (4) sample holder, (5) cryo-cooler, (b) schematic of sample holder with configuration 1 and 2 for Hall and C-V / I-V measurement, and (c) schematic representation of spectral response measurement setup where symbols C, F, M, L and S stand for mechanical chopper, filter, monochromator, lens and sample, respectively.

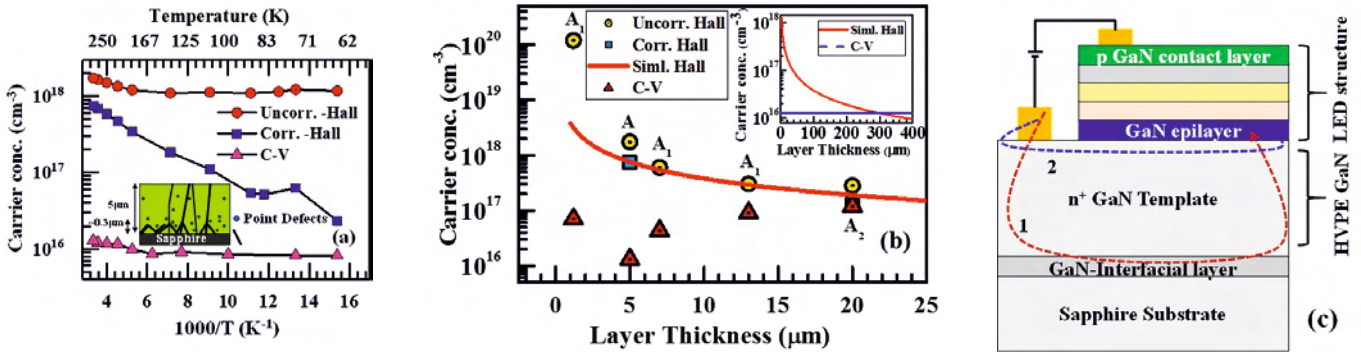

Fig. T.3.2: (a) Temperature dependent carrier concentration values without (Uncorr-Hall) and with (Corr-Hall) two layer model is compared with C-V for HVPE grown GaN templates, (b) carrier concentration values plotted as function of layer thickness for HVPE grown GaN epilayer, where A (5 µm): this work, A1 (1.2, 7, and 13 µm): Ref. [14], and A2 (20 µm): Ref. [15]. Inset shows a comparison of the numerically calculated Hall values with the carrier concentration measured by C-V, and (c) schematic layer structure of a nitride device grown on top of HVPE GaN templates.

On the contrary, MOVPE grown samples are found to be less influenced by interfacial dislocations, which makes them attractive for device fabrication. Further, the impact of dislocations on the electronic transport properties of Au/Ni/GaN Schottky diodes fabricated on HVPE GaN template is evaluated. It is found that one needs to consider the activation of two donors operating in the two separate temperature ranges for understanding the temperature dependence of Schottky junction parameters like barrier height and ideality factor [16]. The origin behind these donors are the fundamental mechanisms associated with: (1) thermionic emission (TE) of carriers originating from bulk donors like Si that dominates at high temperature, and (2) thermionic field emission (TFE) associated with charged dislocations that dominates at low temperature. The understanding developed is therefore critical where dislocations might limit the charge transport in nitride devices grown on such templates as schematically shown in Figure T.3.2(c). One might assume that the charge carrier transport mainly occurs via path-1 through the GaN epitaxial layer/template. However, the charge transport predominantly occurs via path-2 and is going to be severely limited by the dislocations present in the degenerate layer lying at the interface.

4. Fabrication of GaN UV detector

With the knowledge of the electronic transport properties of GaN epilayers, the next step is to fabricate GaN metal-semiconductor-metal (MSM) UV PDs. As described in the previous section that the electronic transport characteristics of HVPE GaN epilayers are largely influenced by the threading dislocations. On the other hand, MOVPE GaN epilayers are found to be free from such limitations. It is therefore obvious that MOVPE GaN epilayers might be a preferred choice for the fabrication of optoelectronic devices. However, a high cost associated with MOVPE GaN epilayers becomes a major factor that compels researchers to look for other alternatives like HVPE GaN epilayers. MSM PDs are made on MOVPE and HVPE GaN epilayers for comparison purpose. The device geometry is shown in Figure T.3.3(a-d). Contrary to the general understanding, it is surprising to note that the photo response of HVPE based PDs is found to be ~3 times higher than that of the MOVPE based devices [17] as shown in Figure T.3.4.

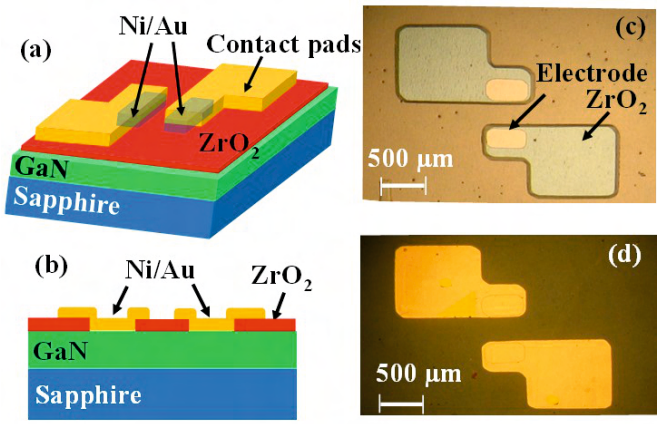

Fig. T.3.3: (a) Schematic diagram showing the device structure, (b) cross-sectional view of the device, (c) optical microscopic image of the device after second step of photolithography prior to metallization where PPR stands for the positive photoresist, and (d) final device subsequent to the metallization and lift-off procedure.

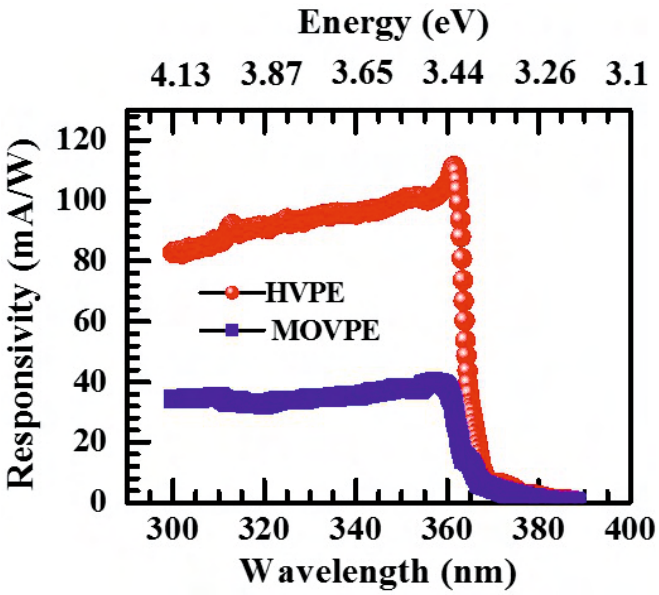

Fig. T.3.4: Room temperature spectral response of GaN MSM PDs.

Further, the overall performance of HVPE based PDs are found to be better than those fabricated on MOVPE GaN, in spite of the variations in device geometry or the operating conditions. It is explained by considering the difference in the depletion layer width, which is primarily determined by the different procedures adopted for the doping of HVPE and MOVPE GaN samples. A large carrier concentration at the edge of the depletion width in MOVPE grown GaN epilayer leads to higher (lower) leakage current (barrier height) despite a low dislocation density. Moreover, Si doping increases the concentration of Ga vacancies, which reduces the minority carrier diffusion length due to the presence of deep level defects [18]. These Ga vacancies trap the photo generated carriers in depletion region leading to the observed reduction in the transient response of PDs fabricated on MOVPE grown sample.

In temperature dependent I-V measurements, the TFE process mediated by carrier tunnelling can be considered as a probable mechanism, which can explain the I–V characteristics shown in Figure T.3.5. The reverse bias current under this model as proposed by Padovani and Stratton [19] can be expressed as:

$$I_{TFE} = I_{TFE,S}\, exp\left(-\frac{qV_R}{\zeta}\right) \quad (1)$$

where, $I_{TFE,S}$ is the saturation current, V_R is the applied bias, and parameter ζ is expressed as $\zeta = E_{00}\left[\left(\frac{E_{00}}{kT}\right) - tanh\left(\frac{E_{00}}{kT}\right)\right]^{-1}$

where, k is the Boltzmann constant, T is the temperature in Kelvin and E_{00} is the characteristic tunnelling energy, which is proportional to $\sqrt{N_D}$.

Thus, a large value of E_{00} indicates about the dominance of TFE mechanism in charge transport. It is observed that I–V characteristics of both the samples can be reasonably fitted by Equation (1) over a wide temperature range, as shown in Figure T.3.5(a & b). The values of E_{00} obtained from the fitting procedure are plotted in Figure T.3.5(c) for both the samples.

A sharp change in the value of characteristics tunnelling energy is seen at ~ 200 K for HVPE GaN as shown in Figure T.3.5(c), which explain the switching of electronic transport mechanism from TE to TFE during the cooling down. On the other hand, TFE is found to be the dominant transport mechanism at all temperature in devices fabricated on MOVPE grown epilayers. The analysis presented here indicates that controlling the density of threading dislocations is not the sole criteria for improving the performance of GaN Schottky PDs, rather one also need to be careful about the density of point defects, which can also marginalize the key figure-of-merits.

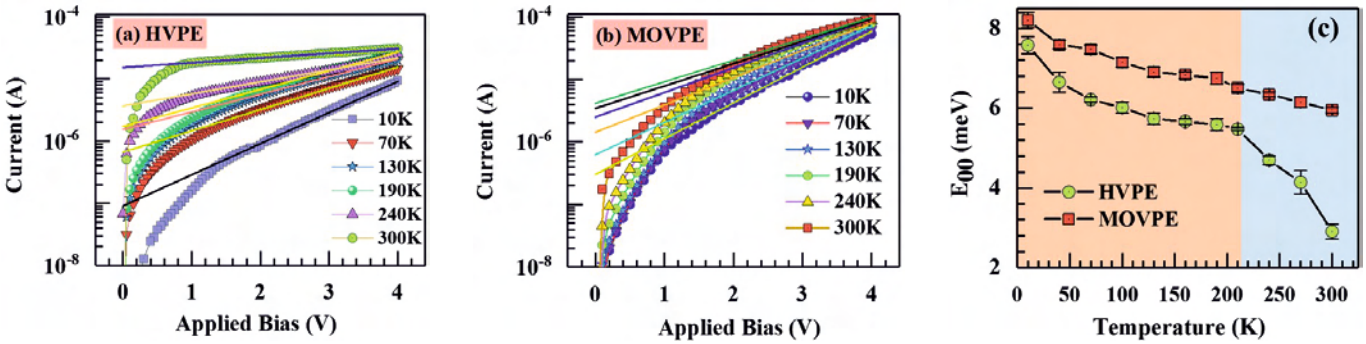

Fig. T.3.5: Temperature dependent I-V characteristics of (a) HVPE, and (b) MOVPE GaN, where the respective solid lines show the corresponding theoretical curves based on the TFE model, and (c) temperature dependence of characteristic tunnelling energy (E_{00}) shown for the two GaN samples, error bars include both the statistical and fitting errors.

5. Improvement in device performance using oxide interlayer

In order to improve the device performance further, GaN based MOS detector is fabricated by including an oxide layer in the device architecture. A thin layer of ZrO_2 (SiO_2) is inserted between the metal and the semiconductor to obtain Au/Ni/ZrO_2 (SiO_2)/GaN MIS PD structure as shown in Figure T.3.6.

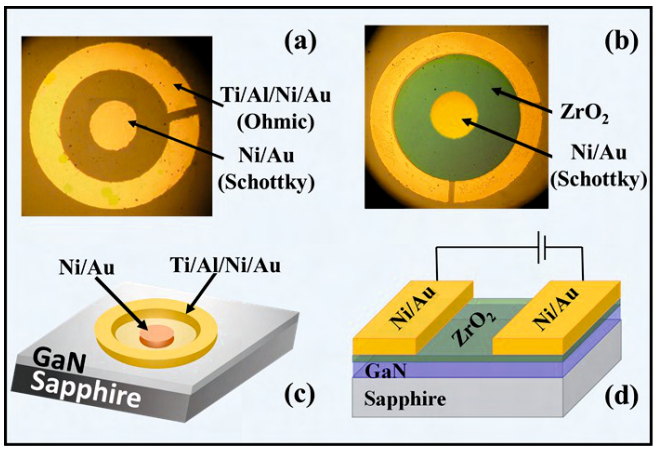

Fig. T.3.6: Optical microscopic image of the device (a) without and (b) with oxide inter layer, (c-d) schematic diagram showing the device structure.

It is observed that the leakage current reduces drastically by 28 (8) times due to insertion of ZrO_2 (SiO_2) leading to a considerable improvement in the photo response as shown in Figure T.3.7(a). The oxide passivated samples show a relatively flat response in shorter wavelength side due to a suppressed surface recombination of photo generated carriers. Moreover, at an optimum ZrO_2 thickness of 3 nm, a high photo responsivity of 27 A/W is achieved as shown in Figure T.3.7(b) along with the fast response of the device with a rise (fall) time of 28 ms (178 ms), respectively [20]. It is also found that the thickness of ZrO_2 layer plays a critical role in controlling the photo-response and transient response of the devices. However, beyond an optimum thickness of oxide interlayer, the device response slows down to 146 ms (256 ms) along with a reduction in responsivity, which is mainly governed by the impediment of hole tunnelling across the oxide layer as schematically represented in Figure T.3.7(c). When the thickness of the oxide layer is low, holes with small energy can tunnel through the barrier. For a larger oxide layer thickness, the tunneling probability reduces, and holes with higher energy will only be able to tunnel through the triangular barrier. Consequently, a low value of photo-response is recorded for larger (>3 nm) values of ZrO_2 layer thickness. It is worth to note that the detectivity (D^*) of PDs with optimized thickness of ZrO_2 interlayer is found to be similar or better than the recently reported state-of-the-art values for visible blind UV GaN PDs with similar dark current as shown in Figure T.3.8.

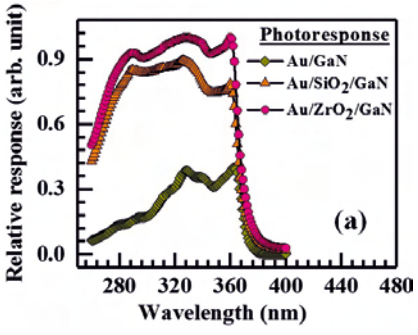

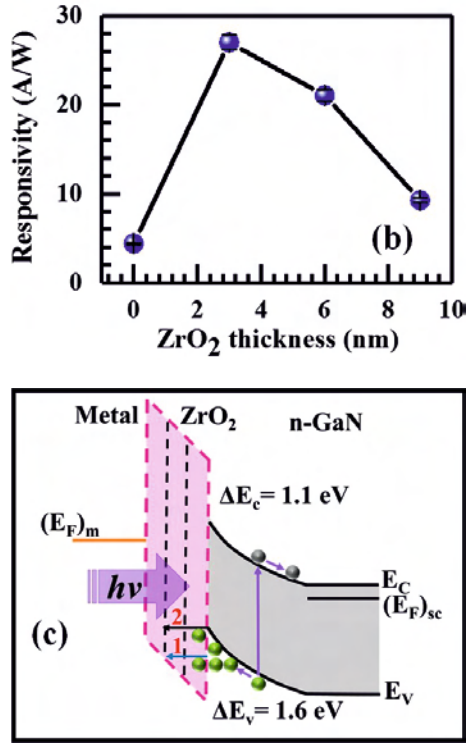

Fig. T.3.7: (a) Relative response of Au/GaN, Au/SiO_2 (ZrO_2)/GaN and Au/GaN devices, (b) responsivity of GaN PDs with different thickness of ZrO_2 layer, and (c) energy band diagram for GaN PDs under reverse bias with varying ZrO_2 thickness (black dashed lines), where arrows 1 (2) represent tunneling through high (low) energy hole traps.

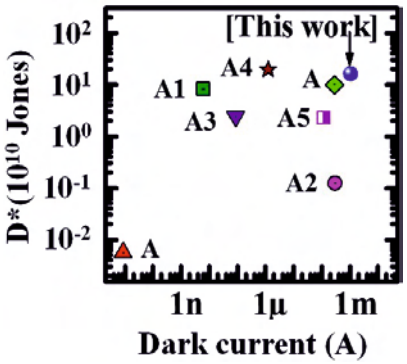

Fig. T.3.8: State-of-the-art values of D versus dark current for GaN UV detectors of the present work along with reported values are plotted for comparison purpose where A: Ref [21], A1: Ref [22], A2: Ref [23], A3: Ref [24], A4: Ref [25], A5: Ref [26].*

6. Importance of dry etching for device fabrication in vertical geometry

Fabrication of an optoelectronic device with smaller geometry requires precise pattern transfer, which can be achieved by photolithography and selective spatial etching of the material. Due to the involvement of sapphire substrate, which is of insulating nature, bottom contacts are to be made on the n-GaN layer.

For fabricating light emitting diodes or PIN PDs based on GaN/sapphire, it is essential to etch part of the sample to expose the bottom n-layer for contact formation and the conduction occurs in vertical geometry. In case of GaN, reactive ion etching (RIE) is a preferred method since wet chemical etchants are not available. However, during this process, several kinds of plasma-induced damages can lead to the creation of lattice defects and dislocations, ion implantation or formation of dangling bonds on the surface [27]. In this section, importance of RIE and its impact on device performance is discussed.

6.1 RIE induced damages in GaN

In order to investigate the impact of plasma etching, the surface morphology of etched GaN epilayers is examined by scanning electron microscopy (SEM). Representative SEM image depicting the surface morphology of GaN epilayer before and after plasma etching with 250 W RF power is shown in Figure T.3.9. The SEM images show that the ion bombardment during dry etching roughens the surface, which indicates that the other material properties may also be altered by the energetic impinging ions. Further, RIE induced damage also impact the optoelectronic properties of GaN epilayers and also the photoresponse of Schottky PDs. The intensity of near band edge photoluminescence peak reduces considerably after dry etching, which indicates the generation of non-radiative recombination centers due to energetic ion bombardment.

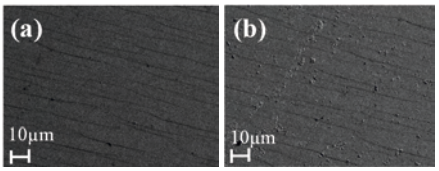

Fig. T.3.9: SEM image of (a) un-etched, and (b) 250 W RF power etched GaN.

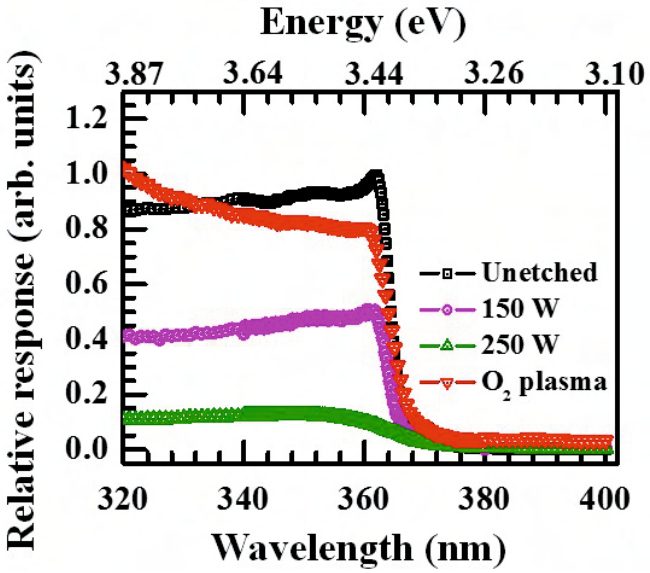

Fig. T.3.10: Plasma etching induced degradation and post etch O_2 plasma treatment induced recovery of photo response of Au/Ni/GaN Schottky detector.

The peak spectral response of Au/Ni/GaN Schottky PD shows up to 90% reduction post plasma etching [27] as shown in Figure T.3.10. Moreover, the surface morphology as well as device response significantly improves in the above band gap region after post etch O_2 plasma treatment. It clearly shows a systematic improvement made in the photo-response of detectors subsequent to the O_2 plasma treatment, which validates the usefulness of the process.

6.2. Fabrication of GaN UV detector in vertical geometry using RIE

After developing an in-depth understanding on the extent of damage created by plasma etching on the surface morphology and optoelectronic properties of GaN and a method of recovery of the damage by O_2 plasma treatment, the immediate aim is to fabricate a GaN PIN detector using RIE. Using the optimized etch parameters, mesa etching is performed to fabricate GaN PIN detector as schematically shown in Figure T.3.11(a). It also presents the depth profile of major dopants, namely Mg for p-type and Si for n-type, present in the epitaxial structure performed using secondary ion mass spectrometry (SIMS) technique.

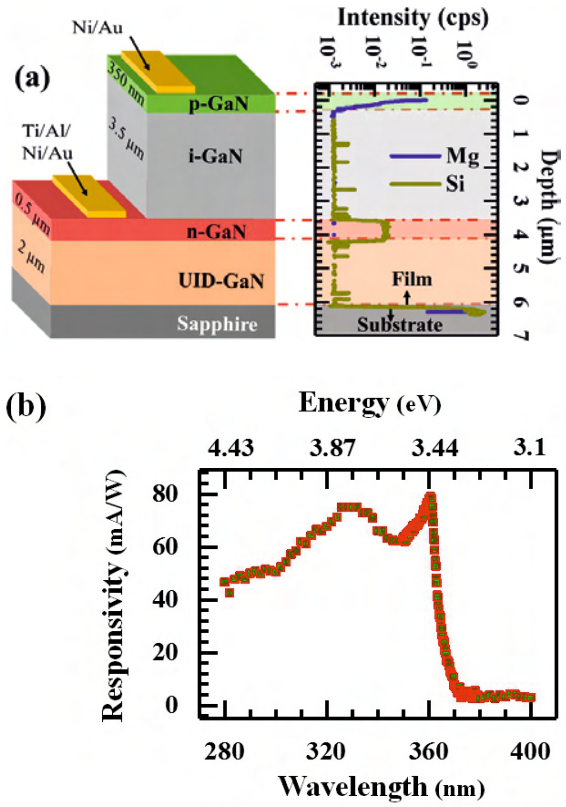

Fig. T.3.11: (a) Schematic diagram of GaN PIN detector along with SIMS profile showing the major dopants profile of Mg and Si for the p and n-GaN layers, respectively (b) room-temperature spectral response of GaN PIN detector at an applied bias of 0.5V.

The spectral response of the detector is recorded over the spectral range of 280-400 nm showing a peak responsivity of 80 mW/A at 362 nm and a high value of D^* of 6×10^{11} Jones as shown in Figure T.3.11(b), which is found to be better than that of GaN MOS detector. The results presented here are helpful in gaining the required understanding of RIE induced damage and also in the minimization of plasma etch induced degradation in optoelectronic properties of GaN epitaxial layer and spectral response of GaN UV PDs.

7. Impact of gamma irradiation on device performance

One of the major aims of the present work is to test the performance of PDs under high radiation environment and the same is discussed in this section. Here, the effect of ^{60}Co gamma irradiation on the electronic transport properties of heavily doped n-type GaN epilayers and Schottky PDs is discussed. A steady rise of carrier concentration in GaN epilayer with increasing irradiation dose is observed. By considering a two layer model, the contribution of interfacial dislocations in carrier transport is isolated from that of the bulk layer for both the pristine and irradiated samples. The bulk carrier concentration is fitted by using the charge balance equation, which indicates that no new electrically active defects are generated by gamma radiation even at 500 kGy dose [28]. The irradiation induced rise of carrier concentration is attributed to the activation of native Si impurities that are already present in an electrically inert form in the pristine sample. This observation is found to be unique, especially for highly conducting samples. It is also seen that the irradiation induced nitrogen vacancies stimulate the diffusion of oxygen impurities, leading to the observed increase of the interfacial carrier concentration. Further, the leakage current of GaN PDs is compared with that of GaAs device with similar background carrier concentration of ~ 10^{18} cm^{-3}. A two order increase in leakage current after irradiation in GaAs PD is observed whereas only a nominal rise of leakage current is observed in case of GaN. This is because GaN has higher displacement energy, which results in lesser number of generation-recombination (g-r) centres after irradiation. Large band gap of GaN further restricts the increase in g-r current, leading to only a nominal increase in leakage current in comparison to GaAs. Further, to investigate the impact of γ irradiation on the charge collection efficiency of GaN based Schottky PDs, the spectral response of pristine and 200 kGy irradiated GaN Schottky photodiodes is compared in the range of 300-400 nm as shown in Figure T.3.12. It is observed that the peak spectral response decreases by 60% after irradiation, which can be attributed to the reduction of charge collection efficiency. However, the photo response partially recovers after 16 hours of irradiation, which is found to recover completely within a day. Such a recovery of spectral response is attributed to the room temperature annealing of irradiation induced defect states, which signifies the compatibility of devices for operation in high radiation zones.

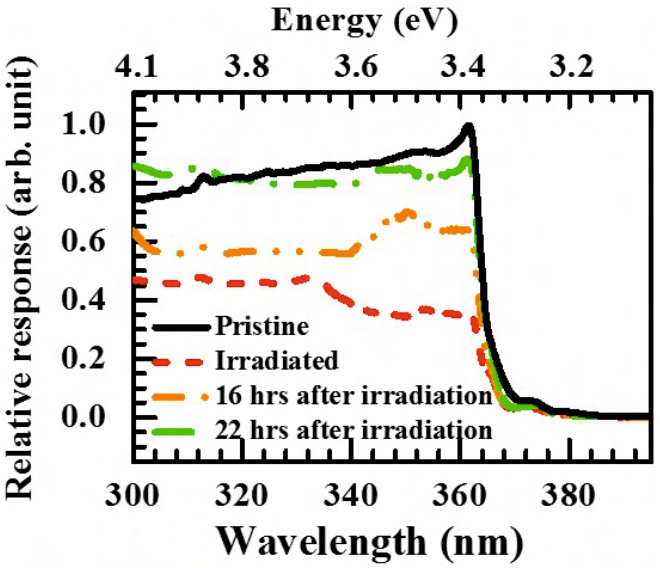

Fig. T.3.12: Photo response of GaN Schottky photo detector after irradiation with ^{60}Co gamma source.

8. Conclusion

In-depth electronic transport measurements have been performed on MOVPE and HVPE-grown GaN epilayers. The presence of a highly conducting interfacial layer was observed in HVPE GaN epilayers. On the other hand, MOVPE GaN epilayers were found to be free from this limitation, which makes them attractive for device development. A method to enhance the detector performance has been demonstrated by the insertion of a thin layer of ZrO_2 forming GaN MIS PDs. The role of ZrO_2 layer thickness was found to be rather critical, where the specific detectivity of the devices were found to be similar, or better than the state-of-the-art values reported in the literature. Further, the role of RIE in the fabrication of smaller devices was discussed where a method to recover the RIE induced damage is demonstrated by using post-etch O_2 plasma treatment. Finally, the GaN detectors were tested under a high dose of gamma irradiation, where a fast self-recovery of the spectral response signifies their usefulness for possible applications in a radiation environment.

Acknowledgements

The present research work has been carried out under the guidance of Dr. T. K. Sharma, Head, Materials Science Section, RRCAT. The author would like to thank Dr. V. K. Dixit, Head, Semiconductor Materials Lab (SML) and Dr. Shailesh K. Khamari for many useful discussions and valuable suggestions. The technical support from Shri U. K. Ghosh, Shri A. K. Jaiswal, Shri A. Khakha, Shri S. Porwal and Shri V. Agnihotri is greatly acknowledged. Author would also like to acknowledge the support of all the SML group members during the entire work. Author also acknowledges Dr. Shankar V. Nakhe, Director, RRCAT for his constant support during the course of this work.

References

[1] C. S. J. Pearton, J. C. Zolper, R. J. Shul, F. Ren, "GaN: Processing, defects, and devices", J. Appl. Phys. 86, 1 (1999).

[2] M. Brendel, M. Helbling, A. Knigge, F. Brunner, and M. Weyers, "Measurement and simulation of top- and bottom-illuminated solar-blind AlGaN metal-semiconductor-metal photodetectors with high external quantum efficiencies", J. Appl. Phys. 118, 244504 (2015).

[3] J. Grant, W. Cunningham, A. Blue, V. O'Shea, J. Vaitkus, E. Gaubas, M. Rahman, "Wide bandgap semiconductor detectors for harsh radiation environments", Nucl. Instr. and Meth. A 546, 213 (2005).

[4] K. Fujito, S. Kubo, H. Nagaoka, T. Mochizuki, H. Namita and S. Nagao, "Bulk GaN crystals grown by HVPE", J. Cryst. Growth 311, 3011 (2009).

[5] A. Chatterjee, V. K. Agnihotri, R. Kumar, S. Porwal, A. Khakha, Jayaprakash G., Tapas Ganguli and T. K. Sharma, "Optimization of the growth of GaN epitaxial layers in an indigenously developed MOVPE system", Sadhana 45, 249 (2020).

[6] S. Nakamura and M. R. Krames, "History of Gallium–Nitride-Based Light-Emitting Diodes for Illumination", Proc. IEEE 101, 2211 (2013).

[7] B. Heying, X. H. Wu, S. Keller, Y. Li, D. Kapolnek, B. P. Keller, S. P. DenBaars, and J. S. Speck, "Defect structure of metal□organic chemical vapor deposition□grown epitaxial (0001) GaN/Al_2O_3", Appl. Phys. Lett. 68, 643 (1996).

[8] H. Amano, N. Sawaki, I. Akasaki, and Y. Toyoda, "Metalorganic vapor phase epitaxial growth of a high quality GaN film using an AlN buffer layer", Appl. Phys. Lett. 48, 353 (1986).

[9] Z. Huang, Y. Zhang, G. Deng, B. Li, S. Cui, H. Liang, Y. Chang, J. Song, B. Zhang, G. Du, "Improvements of epitaxial quality and stress state of GaN grown on SiC by in situ SiNx interlayer", J Mater Sci: Mater Electron 27, 10003 (2016).

[10] A. Chatterjee, S. K. Khamari, R. Kumar, V. K. Dixit, S. M. Oak, and T. K. Sharma, "Dislocations limited electronic transport in hydride vapour phase epitaxy grown GaN templates: A word of caution for the epitaxial growers", Appl. Phys. Lett., 106, 023509 (2015).

[11] O. Lindberg, Proc. "Hall Effect", IRE 40, 1414 (1952).

[12] A. Chatterjee, S. K. Khamari, V. K. Dixit, T. K. Sharma, and S. M. Oak, An Accurate Measurement of Carrier Concentration in an Inhomogeneous GaN Epitaxial Layer from Hall Measurements "Physics of Semiconductor Devices", Environmental Science and Engineering (Springer, 2014), p. 767.

[13] S. M. Sze and K. K. Ng, "Physics of Semiconductor Devices", (John Wiley & Sons, Inc., New Delhi, 2013).

[14] W. Gotz, J. Walker, L. T. Romano, N. M. Johnson, and R. J. Molnar, "Thickness Dependence of Electronic Properties of GaN Epi-layers", MRS Proc. 449, 525 (1996).

[15] D. C. Look and R. J. Molnar, "Degenerate layer at GaN/sapphire interface: Influence on Hall-effect measurements", Appl. Phys. Lett. 70, 3377 (1997).

[16] A. Chatterjee, S. K. Khamari, V. K. Dixit, S. M. Oak, and T. K. Sharma, "Dislocation-assisted tunnelling of charge carriers across the Schottky barrier on the hydride vapour phase epitaxy grown GaN", J. Appl. Phys. 118, 175703 (2015).

[17] A. Chatterjee, S. K. Khamari, R. Kumar, S. Porwal, A. Bose and T. K. Sharma, " Role of threading dislocations and point defects in the performance of GaN-based metal semiconductor-metal ultraviolet photodetectors", Superlattices and Microstructures 148, 106733 (2020).

[18] D. G. Zhao, D. S. Jiang, J. J. Zhu, Z. S. Liu, S. M. Zhang, J. W. Liang, Hui Yang, X. Li, X. Y. Li, and H. M. Gong, "Influence of defects in n-GaN layer on the responsivity of Schottky barrier ultraviolet photodetectors", Appl. Phys. Lett. 90, 062106 (2007).

[19] F. A. Padovani and R. Stratton, "Field and thermionic-field emission in Schottky barriers", Solid-State Electron. 9, 695 (1966).

[20] A. Chatterjee, S. K. Khamari, S. Porwal, and T. K. Sharma, "Role of ZrO_2 Passivation Layer Thickness in the Fabrication of High Responsivity GaN Ultraviolet Photodetectors", Physica Status Solidi: Rapid Research Letters 3, 1900265 (2019).

[21] H. Tian, Q. Liu, C. Zhou, X. Zhan, X. He, A. Hu, X. Guo, "Hybrid graphene/unintentionally doped GaN ultraviolet photodetector with high responsivity and speed", Appl. Phys. Lett. 113, 121109 (2018).

[22] N. Prakash, M. Singh, G. Kumar, A. Barvat, K. Anand, P. Pal, S. P. Singh, S. P. Khanna, "Ultrasensitive self-powered large area planar GaN UV-photodetector using reduced graphene oxide electrodes", Appl. Phys. Lett. 109, 242102 (2016).

[23] A. Gundimeda, S. Krishna, N. Aggarwal, A. Sharma, N. Dilawar Sharma, K. K. Maurya, S. Husale, G. Gupta, "Fabrication of non-polar GaN based highly responsive and fast UV photodetector", Appl. Phys. Lett. 110, 103507 (2017).

[24] N. Aggarwal, S. Krishna, A. Sharma, L. Goswami, D. Kumar, S. Husale, G. Gupta, "A Highly Responsive Self-Driven UV Photodetector Using GaN Nanoflowers", Adv. Electron. Mater. 3, 1700036 (2017).

[25] Ch. Ramesh, P. Tyagi, B. Bhattacharyya, S. Husale, K.K. Maurya, M. Senthil Kumar, S.S. Kushvaha, "Laser molecular beam epitaxy growth of porous GaN nanocolumn and nanowall network on sapphire (0001) for high responsivity ultraviolet photodetectors", J. Alloys Compd. 770, 572 (2019).

[26] H. Tian, Q. Liu, A. Hu, X. He, Z. Hu, X. Guo, "Hybrid graphene/GaN ultraviolet photo-transistors with high responsivity and speed", Optics Express 26, 5408 (2018).

[27] A. Chatterjee, V. K. Agnihotri, S. K. Khamari, S. Porwal, A. Bose, S.C. Joshi and T. K. Sharma, "Peculiarities of the current-voltage and capacitance-voltage characteristics of plasma etched GaN and their relevance to n-GaN Schottky photodetectors", J. Appl. Phys. 124, 104504 (2018).

[28] A. Chatterjee, S. K. Khamari, S. Porwal, S. Kher, and T. K. Sharma, "Effect of ^{60}Co γ-irradiation on the nature of electronic transport in heavily doped n-type GaN based Schottky photodetectors", J. Appl. Phys. 123, 161585 (2018).